

REAL-TIME OBSERVATION OF MICROSTRUCTURE FABRICATION BY MICROPROBE-RHEED/SEM INSTALLED IN MBE CHAMBER

T. Nishinaga

Department of Electronic Engineering, Graduate School of Engineering, The University of Tokyo, 7-3-1 Hongo, Bunkyo-ku, Tokyo 113-8656, Japan

Intersurface diffusion of Ga between facets in MBE of GaAs and real time monitoring of microstructure formation were reviewed. First, the intersurface diffusion was discussed and it was shown that the direction of the diffusion is reversed in varying arsenic pressure. Making use of this it was suggested that the top size of truncated pyramid can be controlled. The formation of pyramids from mesas prefabricated on GaAs (111)B substrate was monitored in real time by microprobe reflection high energy electron diffraction/scanning electron microscopy (microprobe-RHEED/SEM) installed in MBE chamber. It was also demonstrated that after the pyramid with the sharp top was completed the pyramid was again changed to the truncated pyramid by increasing the arsenic pressure. To understand the sharpening process of the truncated pyramid, the calculation basing on inter-surface diffusion model was conducted and the results are compared with the experiments. From the comparison we evaluated diffusion coefficient and incorporation lifetime of Ga adatoms. The lifetime and the diffusion coefficient of (111)B substrate were estimated respectively as 1/70 as small and 50 times as large as that of {110} side wall. The mesa shrinks faster when the arsenic pressure is higher, because Ga adatoms on {110} side wall flow more toward (111)B top and less toward the bottom.

Keywords: Microprobe-RHEED/SEM MBE, Inter-surface diffusion, Microstructures, Real time monitoring, Pyramid

1. Introduction

Low dimensional microstructures like quantum wires and quantum dots have been attracting strong interests for the potential applications, such as semiconductor lasers and single electron devices and extensive studies have been carried out towards the fabrication of such devices. Epitaxial growth is

one of the most hopeful techniques to fabricate low dimensional structures in semiconductors because it gives highly perfect nano-structures with high density. So far many techniques of epitaxial growth have been proposed to be employed for the fabrication of nano-structures such as epitaxial growth on patterned substrate [1-5], selective area epitaxy [6-10], self-assembling growth [11-15] and etc. Among these techniques, the epitaxial growth on patterned substrate is one of the most promising techniques because one can control both the position and the size of the nano-structures.

To control the shape of the microstructures, it is important to understand the elementary growth processes in atomic scale. The surface diffusion is the most important process which governs the appearing and disappearing of a facet. If the surface diffusion occurs from A facet to B facet, B facet grows faster and will disappear. The surface diffusion between surfaces is called inter-surface diffusion and we will review this phenomenon first in the present paper.

Second, the growth of the truncated pyramids which have $\{110\}$ side facets is described [16]. The pyramids were grown from mesas on GaAs (111)B substrate and the change of the shape was observed by microprobe-RHEED/SEM installed in the MBE chamber [17]. The truncated pyramid can be used for the fabrication of dot structure on the top by growing GaAs and AlAs alternately. In the present work, we take pyramid as an example of microstructure and study the behavior of the growth especially the arsenic pressure dependence of the top shrinkage. A theoretical calculation has been conducted taking into account inter-surface diffusion [18].

2. Inter-surface diffusion

When two facets are generated side by side during the growth, Ga atoms diffuse from one facet to the other depending on the growth conditions. We call this intersurface diffusion. If there is a difference in adatom concentration, surface diffusion occurs assuming there is no potential difference nor barrier between the facets. Once intersurface diffusion occurs, one facet grows faster than the other, and the facet growing fast will disappear quickly [17]. Thus, during the growth many facets appear and disappear and only a few facets remain in the final stage of the growth. For the fabrication of nanostructures, one should know relative growth rate among various facets during the growth. However, the growth rate of the facets depends on the growth conditions and hence one should find what is the factor which determines the growth rate.

In the present work, we employed microprobe-RHEED/SEM MBE the detail of which is described elsewhere [19]. Fig. 1 shows the schematic illustration of the MBE. By measuring the growth rate distribution on one facet near the boundary, one can know the direction of the surface diffusion [20,21]. The growth rate distribution can be obtained by microprobe-RHEED by measuring the intensity oscillation. The GaAs substrate which was used for the experiment had grooves with (001) top surface and (111)B side surface. We measured the distribution of the growth velocity on the (001) surface. Instead of measuring the whole distribution, we measured growth rate at 2 points. One is on the facet and close to the boundary and the other is the point on the facet very far from the boundary. We

define each growth rate as R_{corner} and R_{planar} respectively. Fig. 2 shows the results of the measurements. In the figure, closed circle and open triangle denote $R_{\text{corner}}^{(001)} / R_{\text{planar}}^{(001)}$ and $R_{\text{corner}}^{(111)B} / R_{\text{planar}}^{(111)B}$ respectively. Here, we define these normalized growth rates as R_A and R_B respectively.

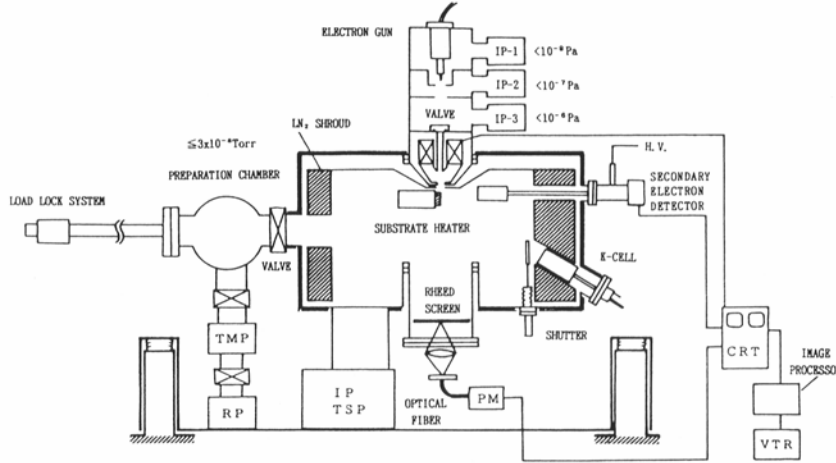


Fig. 1. Schematic illustration of microprobe-RHEED/SEM MBE system.

When the arsenic pressure is low, R_A is larger than unity. As easily understood with Fig. 2, this indicates Ga adatoms diffuse from (111)B to (001). On the other hand, R_B is lower than unity which simultaneously indicates Ga adatoms diffuse from (111)B to (001) being consistent with the direction given by R_A . As the arsenic pressure is increased, R_A decreases and crosses the line of unity at the arsenic pressure of 1.4×10^{-3} Pa, which means the direction of the lateral flow is reversed, namely, from (001) to (111)B. At the same arsenic pressure, R_B also crosses the line of unity from lower side to the higher side. This is very important, since if this does not happen, one can not assume a pure two face intersurface diffusion [20]. As the arsenic pressure is increased, both R_A and R_B keep almost constant values but as the arsenic pressure is further increased, they again cross the line of unity, which means the direction of the diffusion is again reversed. The direction of the diffusion for each arsenic pressure range is given on the top of the figure.

Intersurface diffusion occurs if there is a difference in Ga adatom concentrations between two facets. Here, we assume there is no potential difference nor barrier between these faces. But, there is no evidence for this assumption.

The adatom concentration of Ga, N_{Ga} is proportional to incident flux of Ga, J_{Ga} and τ_{inc} , as follows,

$$N_{\text{Ga}} = J_{\text{Ga}} \tau_{\text{inc}} \quad (1)$$

The incorporation lifetime, τ_{inc} , is inversely proportional to the available number of Ga sites, in other words, to the step density. The step density depends on the number of 2D nucleation and their sizes. Hence, τ_{inc} depends on nucleation rate and the energy barrier for Ga adatoms to enter and to leave

the kink site of the step. There is almost no information for their energies so that we should be satisfied at this moment with qualitative discussions.

Fig. 2 also shows the direction of the intersurface diffusion changes twice as the arsenic pressure is increased. At the second point of directional reversal (higher arsenic pressure side) the reconstruction of (111)B changes from $(\sqrt{19} \times \sqrt{19})$ to (2×2) as arsenic pressure is increased while the reconstruction of (001) is unchanged and keeps (2×4) . It is known that (2×2) reconstruction consists of arsenic trimer which is rather difficult to decompose. Hence, once the (2×2) reconstruction is formed the generation of 2D nucleation might become more difficult which causes the increase of τ_{inc} and hence the increase of Ga adatom concentration.

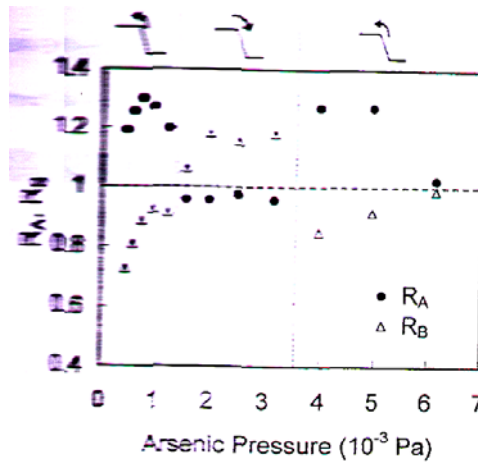


Fig. 2. Normalized growth rate on (001) near the boundary and that on (111)B vs. arsenic pressure. R_A and R_B are $R_{\text{corner}}^{(001)} / R_{\text{corner}}^{(001)}$ and $R_{\text{planar}}^{(111)B} / R_{\text{corner}}^{(111)B}$ respectively.

As for the first point of direction reversal occurring at 1.4×10^{-3} Pa, we have explained in terms of difference in arsenic pressure dependence of τ_{inc} on (001) and (111)B facets [23]. In our previous paper, we extrapolated $P_{As_4}^{-4}$ dependency of τ_{inc} on (111)B but recently we found there is a region in the lower arsenic pressure side where τ_{inc} shows the dependency of $P_{As_4}^{-2}$ [25]. So that up to now, our previous conclusion for $P_{As_4}^{-4}$ dependency of τ_{inc} which is responsible for the directional reversal probably should be changed to $P_{As_4}^{-2}$ dependency. If this is the case, we should assure $P_{As_4}^{-1}$ dependency for (001) surface and $P_{As_4}^{-2}$ dependency for (111)B surface which allows the crossing of τ_{inc} on (111)B and τ_{inc} on (001) at the arsenic pressure of around 1.4×10^{-3} Pa.

3. Fabrication of pyramid and control of the top size[16]

In this section we will describe the formation of the pyramids and the control in the top size of the truncated pyramid by adjusting the direction of the intersurface diffusion. The (111)B GaAs patterned substrates with mesa structures were employed. During the MBE those mesas were changed into the truncated pyramid. The height and the width of the mesa were about $2 \mu\text{m}$ and $4 \mu\text{m}$ respectively as shown in Fig. 3(a). The growth temperature were chosen as 580°C . The growth rate was kept at $0.5 \mu\text{m/h}$ for the first 150 minutes and then decreased to $0.3 \mu\text{m/h}$ to see the change of top size more in detail. The arsenic pressure was chosen at 1.1×10^{-3} Pa.

During the growth, in-situ SEM image was taken and the size of the truncated pyramid was measured from the images after the growth. Fig. 3 shows the real-time photos of the pyramid formation,

and Fig. 3(a), (b), (c), (d), (e), (f) and (g) show respectively the pattern of the substrate before the growth, mesas in the beginning of the growth with $\{221\}$ B facets on the foot of the mesa, $\{110\}$ facets start to cover the mesa, $\{110\}$ facets almost cover the sides, the truncated pyramids with three complete $\{110\}$ side facets, the top size of the truncated pyramid is decreasing and the sharp top pyramids. To see the effect of arsenic pressure on the growth process, the arsenic pressure was increased to 4.7×10^{-3} Pa.

Fig. 3 (h) and (i) show the result. As seen in the figures, the sharp top pyramids change their forms into truncated pyramids. This indicates the direction of surface diffusion was reversed when the arsenic pressure was increased. Hence, by increasing and decreasing the arsenic pressure, one can control the top size of the pyramid.

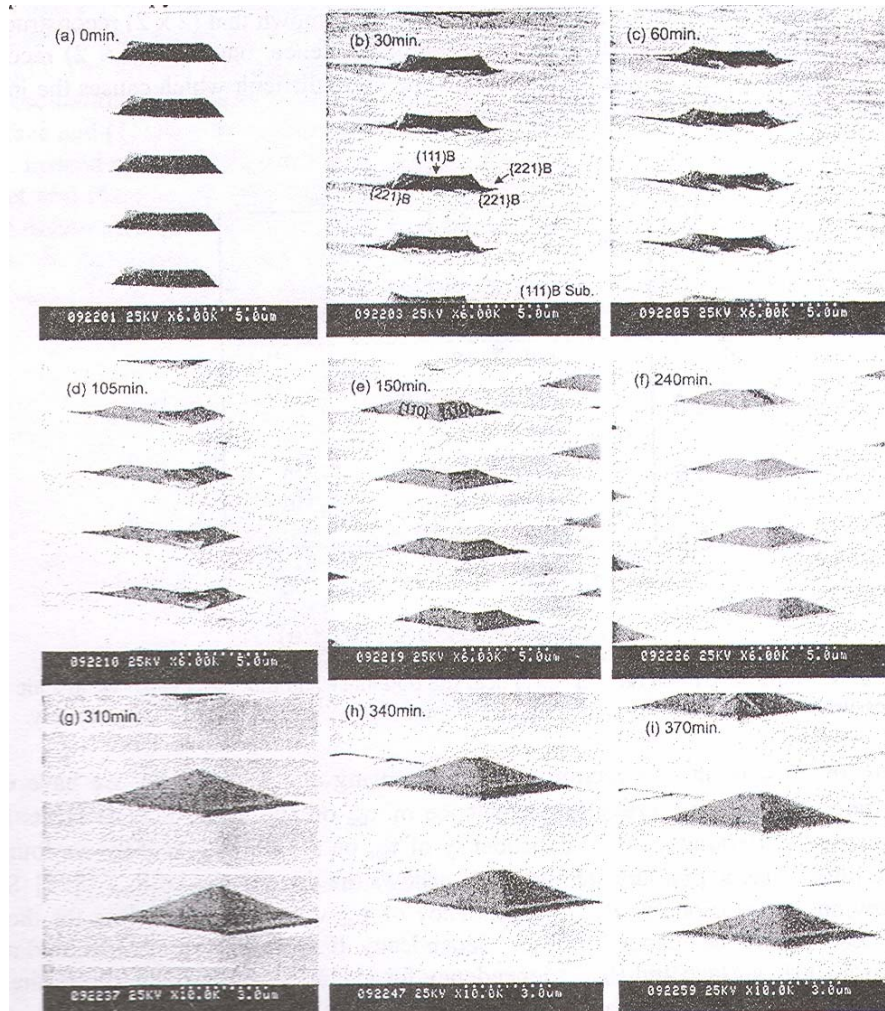


Fig. 3. Photographs of the real-time observations of the faceting and the shrinkage processes on the (111)B patterned substrate. (a) before growth: no special side facet appeared, (b) after 30min: $\{221\}$ B appeared on the bottom of the mesa, (c) after 60min, (d) after 105min, (e) after 150min: the truncated pyramid with three complete $\{110\}$ side facets, (f) after 240min: shrinkage of the top of the truncated pyramid happened, (g) after 310min: the sharp top pyramids were formed and (h) after 340min, (i) after 370 min: by increasing the arsenic pressure, again truncated pyramid appeared.

4. Theoretical calculation [16]

In the following, we propose a simple model based on one-dimensional surface diffusion. On the surfaces of the truncated pyramid, we must consider two-dimensional surface diffusion. But, we can solve this problem by approximating the truncated pyramid as a cone. Fig. 4 shows the coordinates of the cone used in the calculation. In the figure, r , w , s and λ are defined as the distance from the center of the top surface, the half of the top width, the distance on the side wall from the top of the cone and $l \cos \theta$ where l is the side wall length, respectively.

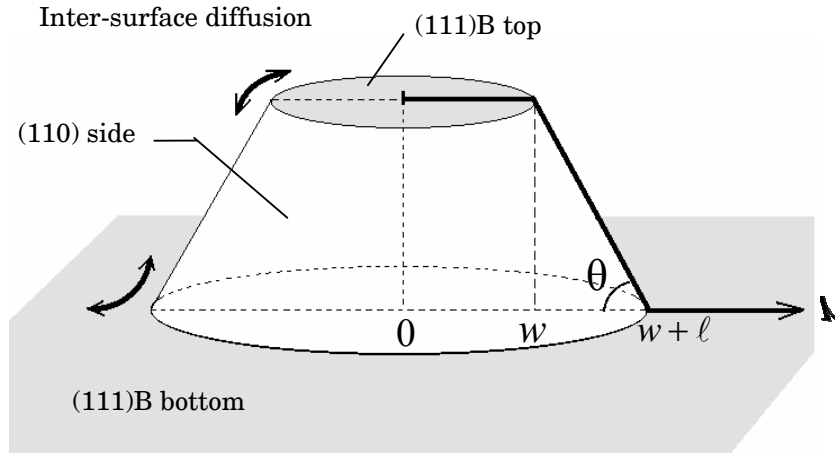


Fig. 4. Coordinates used in the calculation. The truncated pyramid was approximated as a cone.

In the following equations, Ga adatom concentration, diffusion coefficient and incorporation life time on the (111)B top, the bottom and the {110} side surfaces are denoted by the suffices of 'top', 'bott' and 'side', respectively. The equations of the surface diffusion can be given as

$$D_s^{top} \frac{d^2 N^{top}}{dr^2} + \frac{D_s^{top}}{r} \frac{dN^{top}}{dr} - \frac{N^{top}}{\tau_{inc}^{top}} + J_{Ga} = 0 \quad (0 \leq r \leq w),$$

$$D_s^{side} \frac{d^2 N^{side}}{ds^2} + \frac{D_s^{side}}{s} \frac{dN^{side}}{ds} - \frac{N^{side}}{\tau_{inc}^{side}} + J_{Ga} \cos \theta = 0 \quad (w/\cos \theta \leq s \leq w/\cos \theta + l) \quad (2)$$

and

$$D_s^{bott} \frac{d^2 N^{bott}}{dr^2} + \frac{D_s^{bott}}{r} \frac{dN^{bott}}{dr} - \frac{N^{bott}}{\tau_{inc}^{bott}} + J_{Ga} = 0 \quad (w + l \cos \theta \leq r),$$

where N , τ , D_s , and θ are defined as the surface concentration of Ga adatom, its lifetime until incorporation into the crystal, surface diffusion coefficient and angle between (111)B substrate and {110} facet.

From the above equations, the Ga adatom concentration $N(r)$ or $N(s)$ on each surface can be

given as[22]

$$\begin{aligned}
 N^{top}(r) &= T_1 J_0 \left(\frac{ir}{\lambda_{inc}^{top}} \right) + J_{Ga} \tau_{inc}^{top} \quad (0 \leq r \leq w), \\
 N^{side}(s) &= S_1 J_0 \left(\frac{is}{\lambda_{inc}^{side}} \right) + S_2 \operatorname{Re} \left[Y_0 \left(-\frac{is}{\lambda_{inc}^{side}} \right) \right] + J_{Ga} \tau_{inc}^{side} \cos \theta \quad (w/\cos \theta \leq s \leq w/\cos \theta + 1) \\
 \text{and} \\
 N^{bott}(r) &= B_1 \operatorname{Re} \left[Y_0 \left(-\frac{ir}{\lambda_{inc}^{bott}} \right) \right] + J_{Ga} \tau_{inc}^{bott} \quad (w + l \cos \theta \leq r),
 \end{aligned} \tag{3}$$

under the boundary conditions of

$$\begin{aligned}
 D_s^{top} \frac{dN^{top}(r)}{dr} &= 0 \quad (r = 0) \\
 \text{and} \\
 D_s^{bott} \frac{dN^{bott}(r)}{dr} &= 0 \quad (r = \infty),
 \end{aligned} \tag{4}$$

where T_1 , S_1 , S_2 and B_1 are all integral constants and eq.(4) means that there is no lateral flux of Ga adatoms at the center of the top surface because of a symmetry and at the distance far from the pyramid on the bottom surface.

In the present model, we assumed that there is no potential barrier for the surface diffusion across the boundary between (110) and (111)B, which gives the boundary conditions as,

$$\begin{aligned}
 N^{top}(w) &= N^{side}(w), \\
 N^{side}(w/\cos \theta + 1) &= N^{bott}(w + l \cos \theta), \\
 D_s^{top} \frac{dN^{top}(w)}{dr} &= D_s^{side} \frac{dN^{side}(w/\cos \theta)}{ds} \\
 \text{and} \\
 D_s^{side} \frac{dN^{side}(w/\cos \theta + 1)}{ds} &= D_s^{bott} \frac{dN^{bott}(w + l \cos \theta)}{dr}
 \end{aligned} \tag{5}$$

By using the eq.(3) with the boundary conditions of eq.(5), the Ga adatom concentration of each surface can be calculated. Also the growth rate $R(r)$ can be calculated as

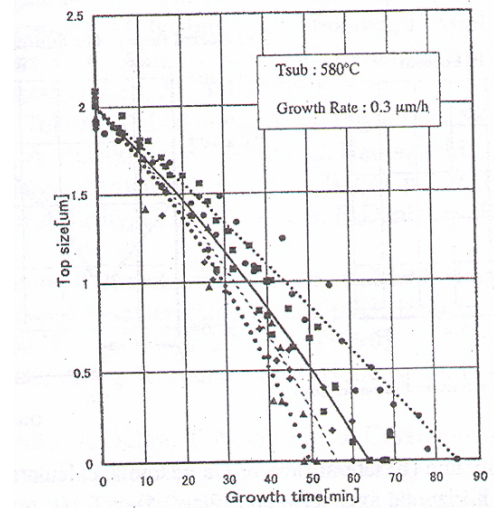
$$\begin{aligned}
 R^{top,bott}(r) &= \frac{N^{top,bott}(r)}{\tau_{inc}^{top,bott}} \\
 \text{and} \\
 R^{side}(s) &= \frac{N^{side}(s)}{\tau_{inc}^{side}}.
 \end{aligned} \tag{6}$$

By repeating this procedure, we can obtain the top size of the truncated pyramid as a function of

the growth time. Fig. 5 shows the calculated results and the experimental data. Parameters used in the calculation were shown in Table 1. In Fig. 5, experimental top size means the length of one side of the top triangle, and the growth time of 0 was defined when top size takes the length of $2\mu\text{m}$, because $\{110\}$ side faceting was completed in all the experiments at this size. Incorporation diffusion length of $(111)\text{B}$ and $\{110\}$ surfaces were measured by Nishinaga *et al.*[23] and Yamashiki *et al.*[26] by microprobe-RHEED oscillation technique. From these experiments, surface diffusion length of $(111)\text{B}$ and $\{110\}$ were chosen respectively as $7.0\mu\text{m}$ for both λ_{inc}^{top} and λ_{inc}^{bott} at $P_{As_4}=6.4\times 10^{-4}\text{ Pa}$ and $8.5\mu\text{m}$ for λ_{inc}^{side} at $P_{As_4}=6.1\times 10^{-4}\text{ Pa}$. Arsenic pressure dependence of the surface diffusion length, $\lambda_{inc} \propto P_{As_4}^{-0.5}$ was employed for both surfaces [25].

Table 1. Parameters used in the calculation.

Experiment (dot)	Calculation (line)						
	P_{As_4} [Pa]	$\lambda_{inc}^{top}, \lambda_{inc}^{bott}$ [μm]	τ^{top}, τ^{bott} [s]	D_S^{top}, D_S^{bott} [cm^2/s]	λ_{inc}^{side} [μm]	D_S^{side} [cm^2/s]	τ^{side} [s]
●	3.64×10^{-4}	9.9	0.098	1.0×10^{-5}	11.7	2.0×10^{-7}	6.9
■	6.38×10^{-4}	7.0	0.050	1.0×10^{-5}	8.3	2.0×10^{-7}	3.5
◆	8.64×10^{-4}	6.1	0.037	1.0×10^{-5}	7.2	2.0×10^{-7}	2.6
▲	1.16×10^{-3}	5.2	0.027	1.0×10^{-5}	6.2	2.0×10^{-7}	1.9

Fig. 5. Time dependence of the top size of truncated pyramid for different As_4 pressures.

Mark and line for each pressure are given in Table 1.

On $\{110\}$ facet, we employed diffusion coefficient of $1.4 \times 10^{-6}\text{ cm}^2/\text{s}$ for D_S^{side} . The reason for the choice of this value is as follows. Yamashiki *et al.* [26] studied the intersurface diffusion of Ga between (001) and (110) facets and found the surface diffusion coefficient on (110) surface is nearly ten times larger than that on (001) surface. Although there is no reliable experimental data for the surface

diffusion coefficient on (001), there is one theoretical work which gave the value of $D_S^{(001)} = 2.0 \times 10^{-8}$ at 600 in the direction which has the lowest diffusivity [24]. These two considerations gave the above value. Ga adatom lifetime τ_{inc}^{side} is given with

$$\lambda_{inc} = \sqrt{D_S \tau_{inc}} \quad (7)$$

and shown in the Table 1.

On (111)B surface, diffusion coefficients D_S^{top} and D_S^{bott} were determined so that calculation agrees with experiment. Ga adatom lifetimes τ_{inc}^{top} and τ_{inc}^{bott} were also obtained from eq. (7). Fig. 5 shows

good agreement between the calculation and the experiment when D_S^{top} and D_S^{bott} were chosen as 1.0×10^{-5} cm²/s. From this calculation, the lifetime and the diffusion coefficient of (111)B substrate were estimated respectively as 1/70 as small and 50 times as large as that of {110} side wall. The value of $D_S^{(111)B} = 1.0 \times 10^{-5}$ cm²/s which shows the best fitting seems very large compared to the value on (001).

Since the surface atomistic configuration is quite different to each other, we cannot eliminate the possibility for (111)B surface to have such high diffusion coefficient. However, as mentioned before, we assumed there is no potential barrier between (110) and (111)B surfaces. The large value of $D_S^{(111)B}$ may include the error which comes from this assumption.

Fig. 6(a) and (b) show respectively Ga adatom density and the lateral flow of Ga adatoms calculated from eq.(3) when top size was 2 μm. As shown in Fig. 6(a), Ga adatom density takes the maximum in the side wall and the maximum values become relatively smaller when the arsenic pressure is increased. Due to the geometrical discontinuities, the lateral flow shows discontinuities in its gradient at the top and bottom boundaries as shown in Fig. 6(b). It is seen in the figure, as arsenic pressure is increased, the lateral flow toward the bottom is decreased while the flow toward the top is increased. On the one hand, when the arsenic pressure is decreased, Ga adatom can diffuse longer, so that the flow toward the bottom is increased and this makes the amount of the flow toward the top small. Basing on this model, we can explain why the mesa shrinks faster when arsenic pressure is higher as shown in Fig. 5. This also suggests that the inter-surface diffusion model is valid for understanding the present experiments.

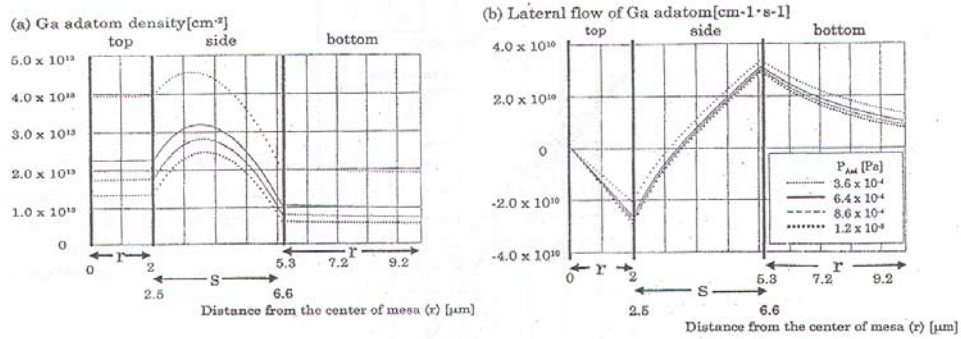


Fig. 6 (a) Ga adatom density and (b) lateral flow of Ga adatoms, calculated from eq.(3), when the top size was $2\mu\text{m}$. The horizontal axis between $r=2(s=2.5)\sim r=6.1(s=6.6)\mu\text{m}$ is taken along the side of the cone.

5. Conclusions

By employing microprobe-RHEED/SEM MBE, intersurface diffusion of Ga between (001) and (111)B surfaces of GaAs was studied as a function of the arsenic pressure. It was shown that the direction of the intersurface diffusion is reversed twice as the arsenic pressure is increased. To utilize the directional reversal of the Ga intersurface diffusion in MBE of GaAs for controlling the size of microstructure the growth of pyramid was conducted. Real time observation of pyramid growth showed that the Ga intersurface diffusion occurs from (110) side facets to (111)B top facet when the arsenic pressure is low while it is reversed when the arsenic pressure is high. It was demonstrated that due to the direction reversal the pyramid with sharp top was changed to the truncated pyramid. This technique can be used to get uniform dot structure on the truncated pyramid even the size of the starting mesa is not uniform.

Theoretical calculations basing on two dimensional diffusion equations were conducted and the results were compared with the experimental changes of the top size of the truncated pyramid. By choosing the appropriate value of the surface diffusion coefficient, we could get a good agreement between the theory and the experiment which shows the intersurface diffusion is the factor that control the facet appearing and disappearing in microstructure fabrication.

Acknowledgments

This work was supported by JSPS Research for the Future Program in the Area of Atomic Scale Surface and Interface Dynamics under the project of "Self-assembling of Nanostructures and its Control" (Project leader, Prof. Y. Arakawa, The University of Tokyo). The author thanks Dr. A. Yamashiki, Dr. D. Kishimoto, Mr. S. Kousai, Mr. T. Ogura, Prof. M. Tanaka and Dr. S. Naritsuka of the University of Tokyo for their helps in the experiments and for the valuable discussions.

References

- [1] E. Kapon, D. M. Hwang, R. Bhat, *Phys. Rev. Lett.* **63**, 430 (1989).
- [2] X. Q. Shen, M. Tanaka, K. Wada, T. Nishinsga, *J. Cryst. Growth* **135**, 85 (1994).
- [3] S. Koshiba, H. Noge, H. Akiyama, T. Inoshita, Y. Nakamura, A. Shimizu, Y. Nagamune, M. Tsuchiya, H. Kano, H. Sakaki, K. Wada, *Appl. Phys. Lett.* **64**, 363 (1994).
- [4] Y. Nakamura, S. Koshiba, M. Tsuchiya, H. Sakaki, *Appl. Phys. Lett.* **59**, 700 (1991).
- [5] A. Madhukar, K. C. Rajkumar, P. Chen, *Appl. Phys. Lett.* **62**, 1547 (1993).
- [6] S. Tsukamoto, Y. Nagamune, M. Nishioka, Y. Arakawa, *Appl. Phys. Lett.* **62**, 49 (1993).
- [7] S. Tsukamoto, Y. Nagamune, M. Nishioka, Y. Arakawa, *J. Appl. Phys.* **71**, 533 (1992).
- [8] C. S. Tsai, J. A. Lebens, C. C. Ahn, A. Nouhi, K. J. Vahala, *Appl. Phys. Lett.* **60**, 240 (1992).
- [9] T. Fukui, S. Ando, *Electron. Lett.* **35**, 410 (1989).
- [10] T. Fukui, S. Ando, Y. Tokura, T. Toriyama, *Appl. Phys. Lett.* **58**, 2018 (1991).
- [11] M. Tabuchi, S. Noda, A. Sakaki, in: S. Namba, C. Hamaguchi, T. Ando (eds.), *Science and Technology of Mesoscopic Structures*, Springer, Tokyo, p.379, 1992.
- [12] D. Leonard, M. Krishnamurthy, C. M. Reaves, S. P. Denbaars, P. M. Petroff, *Appl. Phys. Lett.* **63**, 3203 (1993).
- [13] T. Nishinaga, I. Ichimura, T. Suzuki, in I. Ohdomari, M. Oshima, Hiraki(Eds.), *Control of Semiconductor Interfaces*, Elsevier, Amsterdam, p.63, 1994.
- [14] T. Fukui, H. Saito, *Jpn. J. Appl. Phys.* **29**, L483 (1990).
- [15] O. Brandt, L. Tapfer, K. Ploog, R. Bierworf, M. Hohenstein, F. Phillipp, *Phys. Rev.* **B44**, 8043 (1991).
- [16] S. Kousai, A. Yamashiki, T. Ogura, T. Nishinaga, *J. Cryst. Growth* 198/199, 1119-1124 (1999).
- [17] X. Q. Shen, H. W. Ren, T. Nishinaga, *J. Cryst. Growth* **177**, 175 (1997).
- [18] X. Q. Shen, D. Kishimoto, T. Nishinaga, *Jpn. J. Appl. Phys.* **33**, 11 (1994).
- [19] T. Suzuki, T. Nishinaga, *J. Cryst. Growth* **142**, 49 (1994).
- [20] A. Yamashiki, T. Nishinaga, *Cryst. Res. Technol.* **32**, 1049 (1997).
- [21] T. Nishinaga, A. Yamashiki, X. Q. Shen, *Thin Solid Films* 306 (1997).
- [22] H. Takarabe, Bachelor Thesis, Department of Electronic Engineering, The University of Tokyo (1996).
- [23] T. Nishinaga, X. Q. Shen, D. Kishimoto, *J. Cryst. Growth* **163**, 66 (1996).
- [24] T. Ohno K. Shiraishi, T. Ito, *Mat. Res. Soc. Symp. Proc. Vol. 326*, 27 (1994).
- [25] T. Nishinaga, A. Yamashiki, *Thin Solid Films* 343/344, 495 (1999).
- [26] A. Yamashiki, T. Nishinaga, *J. Cryst. Growth*, 198/199, 1125 (1999).